Published in Physical Review B 54, issue 8, 5893-5900, 1996
which should be used for any reference to this work

Electronic structure of high- and low- temperature $c(2\times2)$-Na/Al(001) phases from angle-scanned ultraviolet photoemission

R. Fasel, P. Aebi, R. G. Agostino, and L. Schlapbach
Institut de Physique, Université de Fribourg, Pérolles, 1700 Fribourg, Switzerland

J. Osterwalder
Physik-Institut, Universität Zürich-Irchel, Winterthurerstrasse, 190, 8057 Zürich, Switzerland

The electronic states of Na on Al(001) have been studied by angle-scanned ultraviolet photoelectron spectroscopy. In the initial stage of Na deposition at room temperature, the Al(001) sp surface state is found to be rapidly quenched. From the linear decrease in intensity with coverage, the scattering cross section for electrons in this zone-center surface state scattering off Na surface impurities has been determined. For the two structurally different $c(2\times2)$ phases formed at low temperature and at room temperature, the surface-state dispersions along the $\overline{\Gamma}\,\overline{M}$ and $\overline{\Gamma}\,\overline{X}$ directions of the surface Brillouin zone have been measured and compared to the corresponding results from the clean Al(001) surface. Opposite energy shifts and distinctly different effective masses have been found for the electronic states in the two $c(2\times2)$ phases.

INTRODUCTION

The termination of the perfect crystal-structure at the surface causes a modification of the bulk electronic band structure reflected by the occurrence of surface resonances and surface states. As these states are confined to the surface, they have a profound influence on its physical and chemical properties. Moreover, these states react very sensitively to external perturbations such as adsorption, disorder, or external fields. Establishing a linkage between the electronic structure of a surface and other surface properties such as the geometrical structure, surface dipole layer formation, dynamical properties, chemical reactivity, or catalytic activity, therefore, is one of the most important goals in surface science. In this work, the changes in surface electronic structure induced by Na adsorption on Al(001) at room temperature and at 150 K are discussed. Different local geometrical structures are formed at these two temperatures, which is clearly reflected in the electronic surface properties.

Due to their prototypical nature and their important role in the development of theories of chemisorption, alkali metal on metal adsorption systems have been extensively studied for a long time.[1] Despite these continuous efforts, it has been realized during the past few years that our understanding of alkali metal on metal adsorption is incomplete. Recent findings of surprising and controversial adsorbate structures have stimulated intense experimental and theoretical work.[2–6] Even though a satisfactory understanding of formerly unexpected and unintelligible phenomena has been gained in many cases, several subjects have remained controversial on the theoretical as well as on the experimental side. A particularly intriguing case is represented by the Na/Al(001) adsorbate system, which has recently attracted considerable interest.[7–11] In contradiction to earlier results,[12,13] it has been shown by high-resolution core-level photoelectron spectroscopy that Na adsorption on Al(001) at room temperature (RT) leads to a disruption of the Al surface and to the formation of a surface alloy.[7] A recent surface-extended x-ray-absorption fine-structure (SEXAFS) study of the RT $c(2\times2)$-Na/Al(001) system at 0.5 ML (ML; 1 ML equals the number of surface Al atoms) coverage proposed Na adsorption beneath a reconstructed surface Al layer,[8] whereas very recent investigations using density-functional theory (DFT) conclude that the adsorption energy of the hollow site is the lowest for very low coverages, and that at a coverage of about 0.15 ML a transition from hollow to substitutional site occupation should occur.[9] Substitutional adsorption in this $c(2\times2)$ structure implies that every second surface Al atom has been kicked out and replaced by a Na atom. From a quantitative x-ray photoelectron diffraction study, the coexistence of Na atoms adsorbed in hollow and in substitutional sites has been proposed,[10] whereas in a quantitative low-energy electron-diffraction (LEED) study adsorption at RT was found to occur in substitutional sites only.[11] There is thus some controversy as to the structure of the RT $c(2\times2)$-Na/Al(001) phase.

Interestingly, the same $c(2\times2)$ LEED pattern as obtained upon Na deposition at RT is also obtained upon deposition of 0.5 ML Na at low temperatures (LT) below 150 K. As in the case of K and Rb on Al(111), it has, however, been shown by high-resolution core-level photoelectron spectroscopy that even though the LEED pattern is not temperature dependent, the local geometry varies with temperature and that the structural transition from the LT $c(2\times2)$ phase to the RT $c(2\times2)$ phase is irreversible.[7] Whereas the local geometry in the RT $c(2\times2)$ phase—and accordingly the nature of the irreversible order-order phase transition—are controversial, there is general agreement in that the LT $c(2\times2)$ structure is a chemisorbed phase where the Na atoms occupy the fourfold hollow sites.[7–9,11]

In order to characterize the surface electronic structure of the two $c(2\times2)$-Na/Al(001) phases and the buildup of the controversial RT $c(2\times2)$ structure, we have investigated these systems by means of angle-resolved ultraviolet photoelectron spectroscopy (ARUPS).[14,15] For Na deposition at RT, normal emission spectra of the Al(001) sp surface state have been measured as a function of Na coverage from 0 ML up to the saturation coverage of 1 ML. A rapid quenching of the Al(001) sp surface state is observed at coverages below 0.2 ML, followed by the build up of lower-binding-energy surface-state features characteristic for the reconstructed RT $c(2\times2)$ phase. A different behavior is observed in the chemisorbed LT phase, where the Al surface state is found to shift towards higher binding energy and to hybridize with Al bulk states. In addition to the opposite energy shift in the two $c(2\times2)$ phases, the surface-state bands are found to be associated with distinctly different effective masses.

EXPERIMENT

The measurements were performed in a VG ESCALAB Mark II spectrometer modified for motorized sequential angle-scanning data acquisition.[16] Photoelectrons excited with Mg $K\alpha$ (1253.4 eV) and He I (21.2 eV) radiation were analyzed with a 150-mm radius hemispherical analyzer. The Al(001) surfaces were prepared by several cycles of Ar^+ sputtering (750 eV) and annealing (500 °C), until no traces of contaminants as judged by core-level photoemission and UPS could be detected. The surface order was checked by LEED and by the detection of the Al(001) surface state. Na was evaporated from a carefully outgassed SAES getter source. Particular care was taken to ensure ultraclean Na deposits. All parts of the evaporation source, except the tiny exit slit, were surrounded with liquid-nitrogen cooled walls. In order to enable a real time characterization of the surface during Na evaporation, very low evaporation rates of about 0.03 ML/min were chosen. In this way, the pressure during evaporation only marginally rose from the base pressure of 1.5×10^{-11} to 2.5×10^{-11} mbar. The sample temperature was measured with a thermocouple in mechanical contact with the sample holder. The temperature gradient from the sample surface to the sample holder was determined in a separate calibration experiment with a thermocouple spot welded onto a dummy sample. Sample temperatures given here are corrected for this temperature difference and are estimated to be correct within ±10 K.

EXPERIMENTAL RESULTS AND DISCUSSION

The Na *KVV* intensity as a function of Na coverage measured with Mg $K\alpha$ radiation *during* Na evaporation onto the Al(001) surface held at RT is shown in Fig. 1. The experimental points of this Na uptake curve are found to follow straight lines with a pronounced change in slope after about 14 min. evaporation. After 33 min. evaporation the saturation coverage is reached and the Na *KVV* intensity quite abruptly levels off. As indicated in Fig. 1, the LEED pattern for the sample at saturation coverage is $(\sqrt{17}\times\sqrt{17})R\pm14°$, and at the coverage corresponding to the change in slope of the Na uptake curve a very sharp $c(2\times2)$ LEED pattern is observed. Since the coverage where the $c(2\times2)$ LEED pattern is most

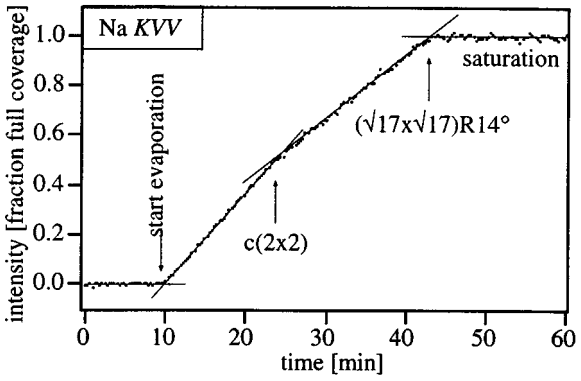

FIG. 1. Na *KVV* Auger electron intensity measured during room-temperature Na deposition on Al(001). The solid lines are linear fits to the respective parts of the experimental curve.

clearly observed is 0.5 ML and the Na *KVV* intensity at saturation is twice the intensity at 0.5 ML, we assign a coverage of 1 ML to the $(\sqrt{17}\times\sqrt{17})R\pm14°$ structure. Interpreting the LEED pattern of this structure in terms of a distorted hexagonal overlayer, a different coverage of 7/8 ML has previously been assigned to this structure by Porteus[17] from geometrical arguments. This value, however, is definitely not compatible with the data shown in Fig. 1.

The strictly linear increase of the Na *KVV* intensity with evaporation time shows that sticking is constant within the different sections and that our evaporation source is very stable. This allows an accurate coverage assignment to the individual spectra obtained during a deposition cycle, even if only the initial and final coverages are known. The respective coverages of the ARUPS spectra shown in Fig. 2 have been assigned accordingly. These normal-emission spectra have been taken with He I radiation during Na deposition onto the Al(001) substrate held at RT. The topmost spectrum is from the clean Al(001) surface, and the last spectrum corresponds to the $(\sqrt{17}\times\sqrt{17})R\pm14°$ structure at saturation coverage. Already for very low coverages, the Al sp surface-state intensity at 2.76-eV binding energy is strongly attenuated, and at a coverage of 0.28 ML this surface state has practically disappeared. Above 0.3 ML a peak at lower binding energy develops and reaches maximum intensity at 0.5-ML coverage. At this coverage, high intensity is furthermore observed at the Fermi edge. For coverages between 0.5 and 1 ML a continuous shift of the 2.31-eV peak to higher binding energies and finally the appearance of two additional weak features at 1.6 and 0.95 eV is observed.

At very low coverages, the adsorbed Na atoms can be viewed as impurities on an otherwise undisturbed surface, which act as scattering centers for the electrons bound in the zone-center surface state (Fig. 3). In this simplified picture, the only influence of the Na atoms is to perturb the surface electronic structure over a range characterized by the scattering cross section σ. For scattering in two dimensions, this surface impurity scattering cross section σ has dimensions of length, and the surface area influenced by the impurity is given by $\pi\sigma^2$ (Fig. 3). In the low coverage regime where the adsorbed impurities are randomly distributed, the surface-state intensity is thus proportional to the unperturbed surface area:

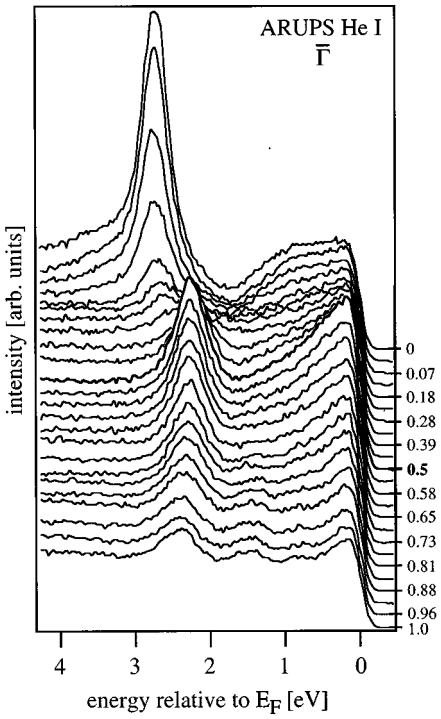

FIG. 2. He I excited normal-emission photoelectron spectra taken during room-temperature Na deposition on Al(001). The coverages corresponding to the individual spectra are indicated in units of 1 ML.

$$I_{SS}(c) \sim \Omega_0 - c\pi\sigma^2 \qquad (1)$$

where Ω_0 is the surface unit-cell area and c is the impurity concentration or coverage. In order to verify whether this linear relationship between surface-state intensity and coverage holds in the present case, we have determined the intensity of the Al(001) sp surface state as a function of Na coverage by background subtraction and integration of the

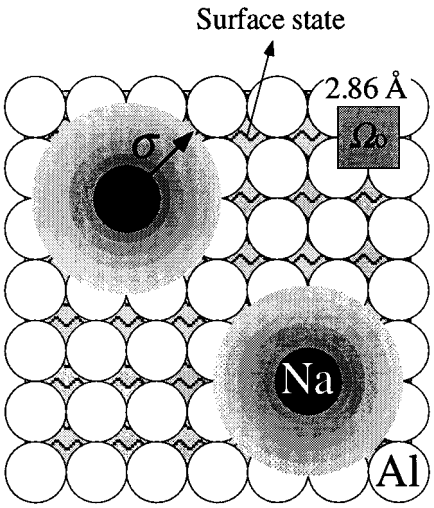

FIG. 3. Schematic illustration of the assumptions underlying Eq. (1). The isolated Na atoms perturb the surface electronic structure over a range σ, and the surface-state intensity is assumed to be proportional to the unperturbed surface area. Ω_0 is the area of the surface unit cell.

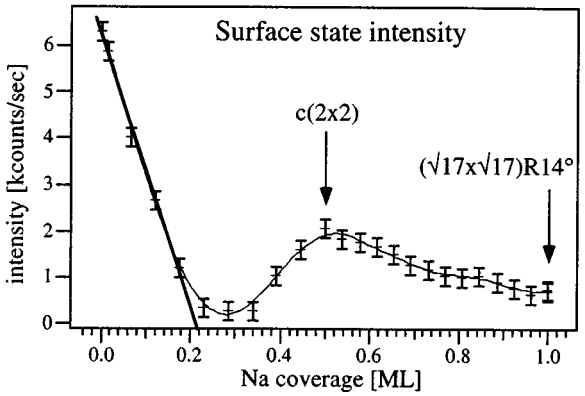

FIG. 4. Intensity evolution of the surface state determined from the spectra shown in Fig. 2. The straight line represents a linear fit to the data in the range from 0 to 0.18 ML.

spectra in Fig. 2. The resulting intensity versus coverage plot is given in Fig. 4. For coverages between 0 and 0.18 ML the data are well fitted by a straight line, and using Eq. (1) the scattering cross section σ can thus be determined. From the slope of the fit indicated by the solid line in Fig. 4 a value of $\sigma = (3.5 \pm 0.2)$ Å is obtained. This value seems reasonable for a metallic system; the range of the screened Coulomb scattering potential is of the order of one unit cell.

A close-up of the spectra shown in Fig. 2 for the coverage regime between 0 and 0.5 ML is given in Fig. 5, where the gradual disappearance of the Al sp surface state at 2.76-eV binding energy and the appearance of the $c(2\times2)$ surface

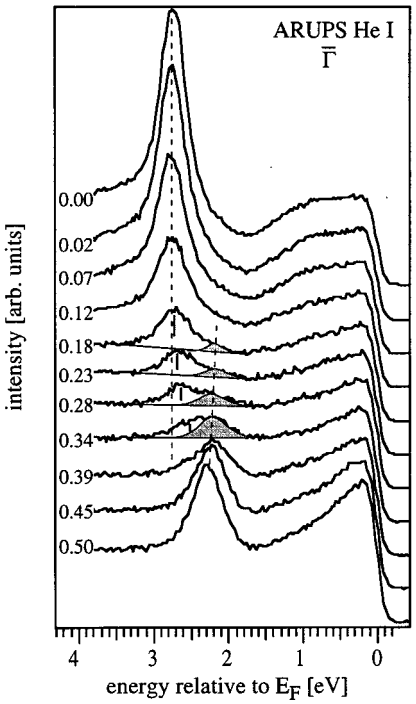

FIG. 5. Expanded view of the 0–0.5-ML spectra of Fig. 2. A shift of the gradually disappearing Al sp surface state towards the Fermi level is observed for coverages above 0.12 ML. As indicated by the shaded areas, the growing of the $c(2\times2)$ surface state starts at a coverage of about 0.18 ML.

state at 2.31 eV with increasing Na coverage are clearly seen. As mentioned previously, the formation and local geometry of the RT $c(2\times2)$-Na/Al(001) structure are somewhat controversial. Based on DFT calculations of the adsorption energies, the occupation of hollow sites has been predicted for coverages up to about 0.15 ML.[9] At this critical coverage a phase transition should occur, where the adatoms switch to substitutional sites and form $c(2\times2)$ islands that increase in size with increasing coverage.

Interestingly, the Al *sp* surface-state intensity decrease (Fig. 4) starts to deviate form the straight-line behavior slightly above 0.15 ML, which is just the coverage predicted for the change in Na-Na interaction from repulsive to attractive.[9] Island growth of the $c(2\times2)$ structure is indicated by the appearance of the $c(2\times2)$ surface-state peak at coverages much below the nominal coverage of 0.5 ML. At 0.18-ML coverage, a very weak shoulder at about 2.2-eV binding energy appears first, overlapping with the residual Al surface-state peak. With increasing coverage this feature continuously becomes more intense and slightly shifts to higher binding energies, until the maximum intensity and a binding energy of 2.31 eV are reached at 0.5-ML coverage. This downward shift is exactly what would be expected for a surface state confined on a growing island; with increasing island size the lateral confinement is released, the formerly discrete surface-state band becomes continuous and shifts to higher binding energies.[18] The inverse behavior is observed for the Al(001) *sp* surface state before dying out: With increasing Na coverage, this state is confined to successively smaller surface patches and therefore shifts to lower binding energies. For confinement on a square two-dimensional island, the critical island width below which the surface state is completely depopulated is given by $\sqrt{2}\lambda_F/2$,[19] which in the present case is of the order of 5 Å. This means that islands as small as a few unit cells can support a surface state, and island formation can, therefore, be detected by ARUPS much before the corresponding LEED pattern is observed.

The observations made up to here can be summarized as follows: At very low coverages below 0.15 ML the Na atoms are randomly distributed over the surface, perturbing the electronic structure of the substrate surface over a range of 3.5 Å. Island formation starts at a coverage of about 0.18 ML, and these $c(2\times2)$ islands continuously grow in size up to a coverage of 0.5 ML. The low binding energy of the surface state at 2.31 eV indicates substitutional site occupation in the RT $c(2\times2)-$Na/Al(001) phase, in agreement with results from other methods.[7,9,11,20] Alkali-metal adsorption in hollow sites (as well as in the other on-surface sites) results in a downward shift of the surface state, because of charge transfer from the adsorbate to the substrate. This geometry can thus be ruled out for the $c(2\times2)$ islands. It can, however, not be decided whether the system additionally contains Na atoms trapped in the metastable hollow site,[10] in patches small enough to prevent the formation of a surface state.

A comparison of the normal-emission spectra from the clean Al(001) surface, the RT $c(2\times2)$-Na phase, and the LT $c(2\times2)$-Na phase is given in Fig. 6. The different local geometrical structures of the two $c(2\times2)$ phases are clearly reflected in their electronic structures. In agreement with expectations for the hollow site geometry, the surface state in the LT $c(2\times2)$ phase is found to be shifted to higher binding

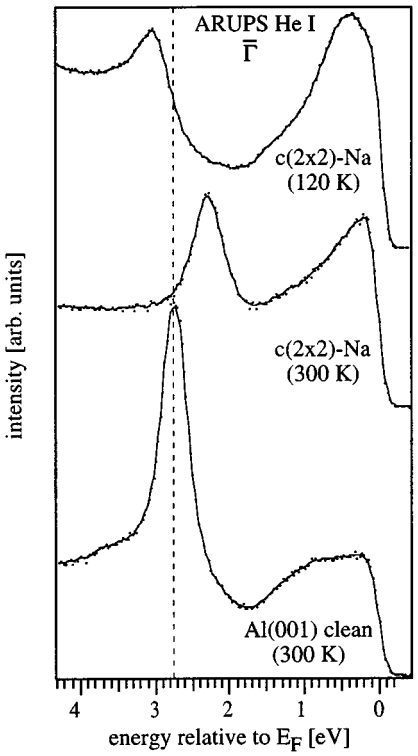

FIG. 6. He I excited normal-emission photoelectron spectra from Al(001), the RT $c(2\times2)$-Na/Al(001) phase and the LT $c(2\times2)$-Na/Al(001) phase.

energies. A second state close to the Fermi level (~0.4-eV binding energy) is observed with high intensity. Enhanced intensity at the Fermi level is also observed in the spectrum from the RT $c(2\times2)$ phase, which might be explained by a state right at the Fermi edge or by an unoccupied state centered slightly above the Fermi level. Similar features close to the Fermi energy have been observed for related systems in photoemission[21] and in metastable deexitation spectroscopy,[22] and have been interpreted as emission from the alkali *s* level.

In order to further characterize these states, we have performed polar scans along the Γ *M* and Γ *X* directions of the Al(001) surface Brillouin zone (SBZ) (Fig. 7), recording at each angular setting the entire photoelectron spectrum between -0.4 and 4.3 eV binding energy. The data sets $I(E_i,\vartheta)$ have then been mapped onto a regular $(E_i,k_\parallel)$ grid and visualized as gray-scale plots with black corresponding to maximum intensity. The dispersion plots obtained in this manner from Al(001), the LT $c(2\times2)$-Na/Al(001) phase and the RT $c(2\times2)$-Na/Al(001) phase are shown in Fig. 8. For all three systems, a free-electron-like dispersion of the zone-center surface state along the Γ *M* and Γ *X* directions is observed. As indicated by the white dashed lines, the dispersion of these states can be well fitted by parabolas of the form

$$E(k_\parallel)=E_0+\frac{\hbar^2}{2m^*}k_\parallel^2. \qquad (2)$$

In order to locate precisely the position of the bands, fits have been performed on the $k_\parallel$ axis rather than on the energy axis, which avoids the problems involved with ill-defined

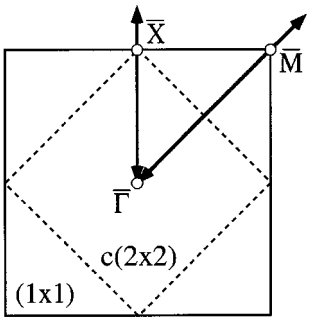

FIG. 7. Surface Brillouin zones corresponding to Al(001) (continuous lines) and $c(2\times2)$-Na/Al(001) (dashed lines). High-symmetry points of the Al(001) surface Brillouin zone are indicated.

lineshapes. The values for the effective masses m^* obtained from the parabolic fits to these bands, the locations of the Fermi-level crossing k_F, and the band energies E_0 are given on the right-hand side of each dispersion plot (Fig. 8). In all cases, the effective mass is found to be isotropic. The band energy of 2.76 eV and the effective mass of $1.18m_e$ determined for the *sp* surface state of the clean Al(001) surface are in good agreement with earlier data. The corresponding values determined by Levinson, Greuter, and Plummer[23] are 2.75 eV and $1.18m_e$, 2.8 eV, and $1.03m_e$ were determined by Gartland and Slagsvold,[24] and 2.75 eV and $1.02m_e$ were found by Hansson and Flodström.[25]

As schematically shown in Fig. 7, the $c(2\times2)$ real-space periodicity is associated with a SBZ half as large as the (1×1) SBZ. Whereas the periodicity along ΓX is unchanged, the $c(2\times2)$ SBZ boundary results in a periodicity doubling along ΓM. In the dispersion plots for the two $c(2\times2)$-Na/Al(001) phases (Fig. 8, center and bottom), this zone boundary of the $c(2\times2)$ SBZ is indicated by a dashed vertical line at $k_{\|}=0.5$. Contrary to the expectation for a Na derived surface state, the LT $c(2\times2)$ surface state does *not* have the periodicity of the $c(2\times2)$ SBZ, but is rather observed to disperse across the $c(2\times2)$ SBZ boundary up to the Fermi level. At a closer look, a very weak band, maybe resulting from surface Umklapp processes, can be recognized

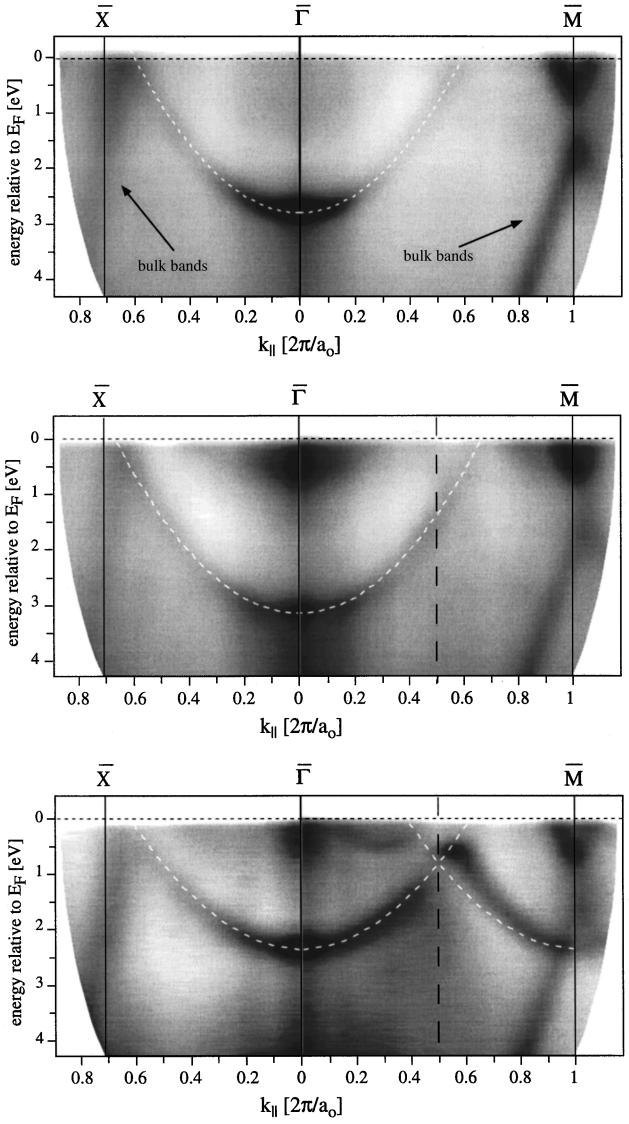

FIG. 8. Dispersion plots from (a) clean Al(001); (b) the LT $c(2\times2)$-Na/Al(001) phase; and (c) the RT $c(2\times2)$-Na/Al(001) phase. These plots represent a series of energy spectra taken on a dense grid of polar angles along the ΓM and ΓX directions of the Al(001) surface Brillouin zone. The representation is in a linear gray scale with low intensities in white and high intensities in black. The white dashed parabolas centered around the Γ points represent the fits to the surface-state bands. Effective mass, Fermi-level crossing, and band energy obtained from these fits are indicated on the right-hand side of each plot.

in the second $c(2\times2)$ SBZ. This state (which is actually located outside the projected volume band gap and is more correctly termed a surface resonance—see below), therefore, cannot be explained as a Na-derived state, but is rather due to the Al(001) surface state modified by the adsorbate. Due to the additional charge from the Na atoms adsorbed in the hollow sites the Al surface state becomes further populated, which results in a downwards shift of the band energy. The charge density distribution of this state, however, does not seem to be modified by the $c(2\times2)$ periodicity of the overlayer. The intense peak at about 0.4 eV binding energy at Γ (Fig. 6, top), however, is well explained by a Na $3s$ derived state. In going along Γ M and Γ X, it shifts towards the Fermi level and decreases in intensity [Fig. 8(b)]. At $k_{\|}\approx0.2$ this peak disappears and reappears in the second $c(2\times2)$ SBZ at $k_{\|}\approx0.8$. These observations are consistent with emission from a partially occupied two-dimensional Na $3s$-derived band. We thus conclude that the LT $c(2\times2)$-Na layer exhibits metallic behavior.

A quite different situation is encountered in the RT $c(2\times2)$ phase (Fig. 8, bottom). The surface state from this phase (band energy 2.31 eV at Γ) disperses slowly towards the Fermi energy, but before reaching the $c(2\times2)$ SBZ boundary, it disappears at $k_{\|}\approx0.45$, reappears in the second $c(2\times2)$ SBZ where it disperses downwards, and finally levels off at M at an energy of 2.31 eV. Apart from the fact that the two branches of this state in the first and second $c(2\times2)$ SBZ are not quite symmetric with respect to the zone boundary (see below), the proper symmetry of the $c(2\times2)$ SBZ is respected. For substitutional site occupation, however, every second top-layer substrate atom is missing, and a $c(2\times2)$ periodicity is, therefore, expected for an Al-derived state of this surface as well. Considering an effective mass as large as $1.55m_e$ as improbable for a surface state of a chemisorbed Na layer, we associate the zone-center surface state of the RT $c(2\times2)$ phase to the Al(001) surface with $c(2\times2)$ vacancies created by the substitutionally adsorbed Na atoms. In agreement with this, recent DFT calculations have identified an occupied feature in the adsorbate-induced density of states at about 2 eV below the Fermi level to be largely due to the Al structure.[2] The relatively large effective mass of the electrons within this surface-state band may reflect the fact that directional bonds are formed between Al atoms of the uppermost layer and their four nearest-neighbor atoms in the layer underneath.[2,9] In contrast to the LT $c(2\times2)$ phase where strong emission from a two-dimensional Na $3s$-derived band is observed, intensity near the Fermi level is only observed at $k_{\|}$ values very close to the Γ point of the first SBZ. If this feature is interpreted in terms of emission from a Na $3s$-derived band, it must be concluded that its occupancy is very low. Finally, it is noted that in the dispersion plot for the RT $c(2\times2)$ phase an additional state is seen to disperse around $k_{\|}\approx0.3$ along Γ M, with an energy at the bottom of the band of about 0.5 eV.

In the discussion given above, the observed electronic states have been termed ''surface states'' in the general sense that they are in relation with the particular surface electronic structure. Strictly speaking, a distinction between ''true'' surface states and surface resonances has to be made. True surface states are restricted to regions where no bulk states of the same symmetry and quantum number exist (gaps in the projected bulk band structure). The wave function of a surface state, therefore, cannot mix with any bulk wave function, and the state is confined to the very surface region of the crystal. The opposite is true for a surface resonance, which may also be viewed as a modification of the wave function of a bulk electronic state with an enlarged amplitude in the surface region of the crystal. For the case of aluminum, a hybridization band gap exists at the X point of the bulk band structure such that there are no bulk states between roughly 2.0 and 3.0 eV below the Fermi level.[23] This bulk band gap results in a gap in the projected band structure at Γ in the SBZ of Al(001); thus a surface state can exist there. In the following, the nature of the states observed in Fig. 8 with regard to their location within the projected bulk band structure is discussed.

The experimental dispersion plot for the clean Al(001) surface is compared in Fig. 9 with two calculations of the Al(001) surface-state dispersion, taken from Ref. 26 and Ref. 27. The (001) projected bulk band structure is represented by the gray-shaded areas [Figs. 9(b), 9(c)]. In both calculations a gap at Γ is found to be between 1.5 and 2.9 eV below the Fermi level, reaching out to $k_{\|}\approx0.5$ along Γ M and to $k_{\|}\approx0.35$ along Γ X. An additional narrow gap extending from about 4.55 eV at X up to about 1.5 eV at $k_{\|}\approx0.35$ along Γ X is seen in these calculations. In good agreement with the experimental results shown in Fig. 9(a), both calculations find a parabolic surface-state band close to the bottom of the gap at Γ. Even though this band leaves the gap when approaching the Fermi level and therefore becomes a surface resonance, the mixing with bulk bands seems to have no—or only marginal—influence on its parabolic dispersion and lifetime. Both, the energy location of this state and its effective mass resulting from the two calculations, agree well with the experimental values of 2.76 eV and $1.18m_e$, respectively. From the DFT calculation[26] shown in Fig. 9(b) values of 2.67 eV and $1.11m_e$ are found, and a band energy of 2.84 eV is obtained from the self-consistent pseudopotential calculation[27] shown in Fig. 9(c). The surface resonance close to M found in the DFT calculation [Fig. 9(b)] is not seen experimentally [Fig. 9(a)].

In Fig. 10, the experimental dispersion plots from the two $c(2\times2)$-Na/Al(001) phases are compared to a self-consistent pseudopotential calculation assuming Na adsorption in the fourfold hollow sites.[27] The location of the gap according to the DFT calculation[26] is schematically indicated in these plots. It can be seen from Fig. 10(a) [LT $c(2\times2)$ phase] that the state showing parabolic dispersion around Γ is located entirely outside the gap, and it thus represents a surface resonance rather than a true surface state. In the pseudopotential calculation shown in Fig. 10(b), this surface resonance is found at somewhat higher binding energies than experimentally observed, which may be due to the small vertical Na-Al separation of 2.05 Å used for these calculations [experimental value 2.57 Å (Ref. 11)]. The charge-density distribution of this surface resonance at Γ has been found to be localized mainly above the topmost Al atoms, very similar to the one of the surface state for Al(001). A Na-derived state, the charge density of which is localized mainly between the Na layer and the second Al layer is found in the calculations with an energy of 0.1 eV at Γ [continuous line in Fig. 10(b)], which may correspond to the Na $3s$-derived state observed

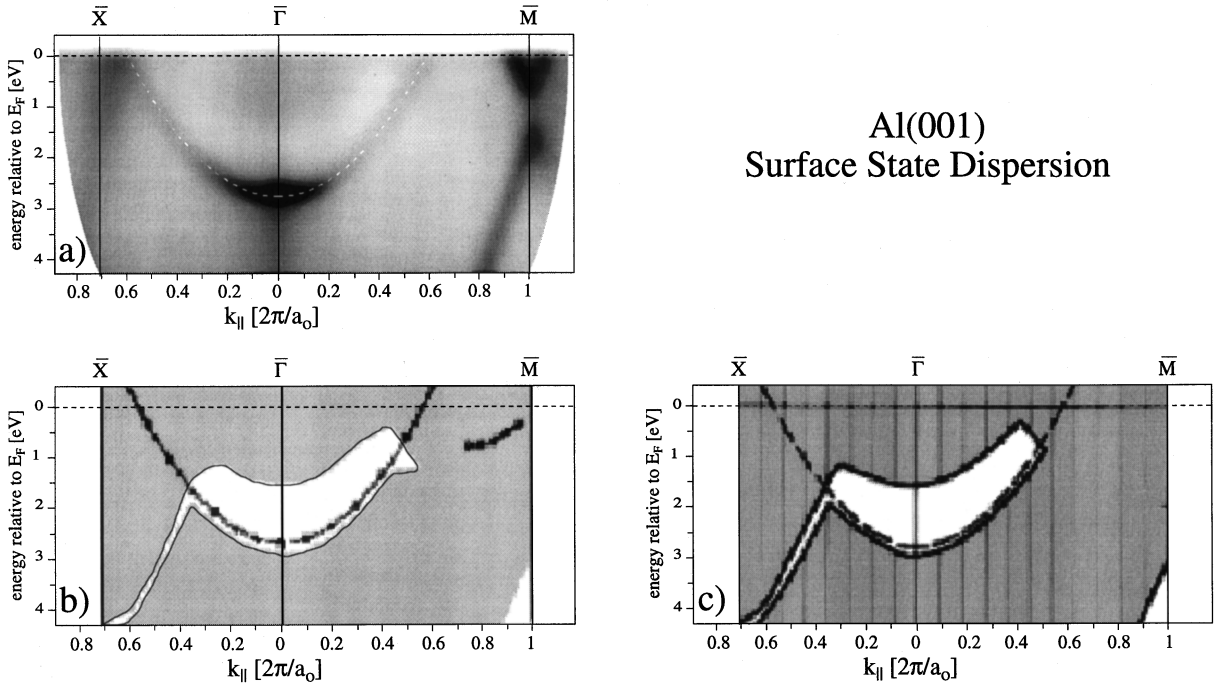

FIG. 9. Experimental dispersion plot from Al(001) (a) compared with theoretical calculations by Heinrichsmeier, Fleszar, and Eguiluz (Ref. 26) (b) and by Chulkov and Silkin (Ref. 27) (c).

in Fig. 10(a) at 0.4 eV below the Fermi level. A few notable differences between this calculation and the experimental dispersion plot from the LT $c(2\times2)$ phase can be noted. In the calculation, the surface resonance discussed above is found to be backfolded into the first SBZ at the $c(2\times2)$ zone boundary, whereas dispersion all the way up to the Fermi level is experimentally observed. An additional surface resonance dispersing upwards from $\overline{X}$ is found in the calculation, but not seen in the experiment.

As mentioned above, the two branches of the zone-center surface state from the RT $c(2\times2)$ phase are not quite symmetric with respect to the $c(2\times2)$ SBZ boundary. In Fig. 10(c) it is seen that along $\overline{\Gamma}\,\overline{M}$, this state is located well inside the gap up to the $c(2\times2)$ SBZ boundary where the gap

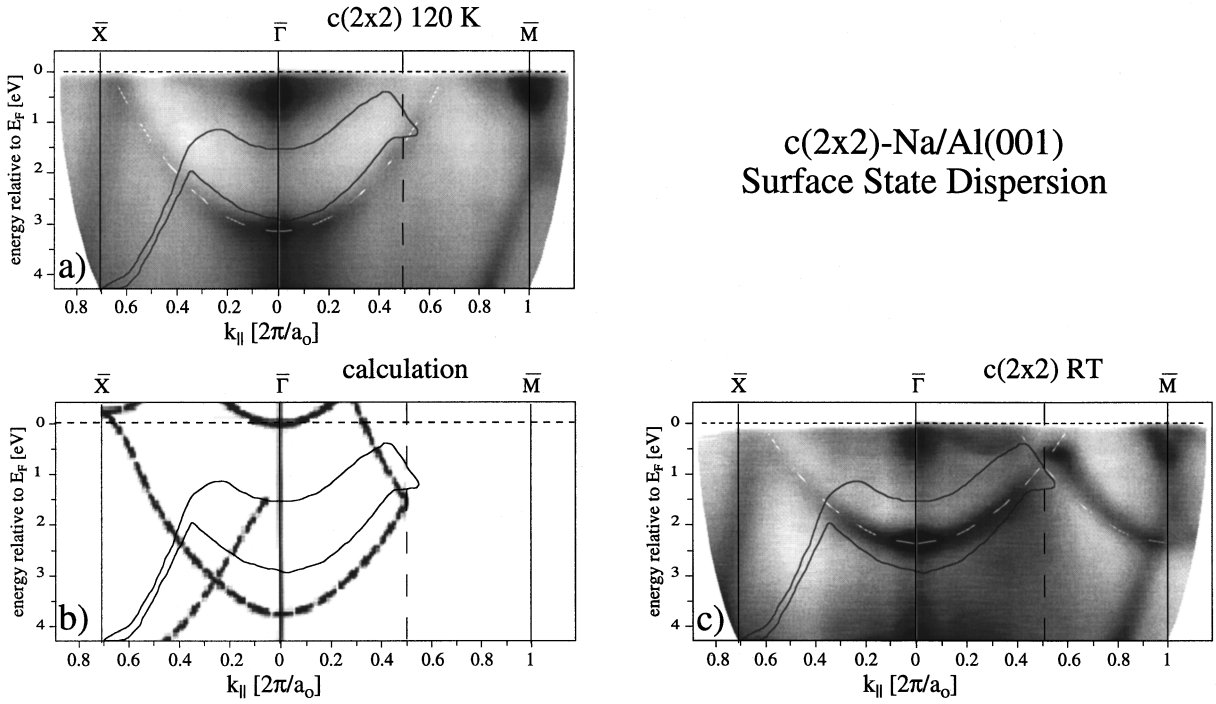

FIG. 10. Experimental dispersion plots from the LT $c(2\times2)$-Na/Al(001) phase (a) and the RT $c(2\times2)$-Na/Al(001) phase (c) compared with a theoretical calculation for Na adsorbed in hollow sites by Chulkov and Silkin (Ref. 27) (b). The location of the band gap according to the calculation by Heinrichsmeier, Fleszar, and Eguiluz (Ref. 26) is indicated in the plots.

disappears. In the second SBZ this state becomes a surface resonance, and strong hybridization with bulk states may modify its dispersion, rendering this branch asymmetric with respect to the one in the first SBZ. Unfortunately, we do not know of any calculation of the RT $c(2\times2)$-Na/Al(001) surface electronic structure. Given the controversial structural results regarding this phase, a comparison of the experimental data shown in Fig. 10(c) with a state-of-the-art surface electronic structure calculation would be most interesting.

CONCLUSIONS

The surface electronic structures of the two $c(2\times2)$-Na/Al(001) phases have been investigated by means of angle-scanned UPS. In the very low coverage regime, the adsorbed Na atoms are found to perturb the surface electronic structure over a range of $\sigma=(3.5\pm0.2)$ Å. For Na deposition at room temperature, the formation of $c(2\times2)$ islands is observed to begin at a coverage of about 0.18 ML. A surface state with a relatively large effective mass of $1.55m_e$ and an energy of 2.31 eV is found for the room temperature $c(2\times2)$ phase. It is attributed to the Al top layer $c(2\times2)$ vacancy structure rather than to the adsorbate layer. In the second $c(2\times2)$ SBZ strong hybridization of this state with bulk bands is observed. Due to the additional charge supplied by the Na atoms in the hollow sites, the Al-derived surface state in the LT $c(2\times2)$ phase is shifted downwards with respect to its energy on the clean Al(001) surface. Even though this state is located outside the gap and has resonant character, its dispersion and lifetime appear unaffected by the mixing with bulk bands. An effective mass of $1.29m_e$ and a band energy of 3.12 eV have been determined for this LT $c(2\times2)$ surface resonance.

ACKNOWLEDGMENTS

The authors acknowledge helpful discussions with T. Greber. Skillful technical assistance was provided by E. Mooser, O. Raetzo, F. Bourqui, and H. Tschopp. This project was supported by the Fonds National Suisse pour la Recherche Scientifique.

[1] An extensive source of references and reviews of many aspects of alkali-metal adsorption can be found in *Physics and Chemistry of Alkali Metal Adsorption*, edited by H. P. Bonzel, A. M. Bradshaw, and G. Ertl (Elsevier, Amsterdam, 1989).
[2] C. Stampfl and M. Scheffler, Surf. Rev. Lett. **2**, 317 (1995).
[3] J. N. Andersen, Surf. Rev. Lett. **2**, 345 (1995).
[4] R. Fasel and J. Osterwalder, Surf. Rev. Lett. **2**, 359 (1995).
[5] R. D. Diehl and R. McGrath, Surf. Rev. Lett. **2**, 387 (1995).
[6] H. Over, H. Bludau, M. Gierer, and G. Ertl, Surf. Rev. Lett. **2**, 409 (1995).
[7] J. N. Andersen, E. Lundgren, R. Nyholm, and M. Qvarford, Phys. Rev. B **46**, 12 784 (1992).
[8] S. Aminpirooz, A. Schmalz, L. Becker, N. Pangher, J. Haase, M. M. Nielsen, D. R. Batchelor, E. Bøgh, and D. L. Adams, Phys. Rev. B **46**, 15 594 (1992).
[9] C. Stampfl, J. Neugebauer, and M. Scheffler, Surf. Rev. Lett. **1**, 222 (1994).
[10] R. Fasel, P. Aebi, J. Osterwalder, L. Schlapbach, R. G. Agostino, and G. Chiarello, Phys. Rev. B **50**, 14 516 (1994).
[11] W. Berndt, D. Weick, C. Stampfl, A. M. Bradshaw, and M. Scheffler, Surf. Sci. **330**, 182 (1995).
[12] B. A. Hutchins, T. N. Rhodin, and J. E. Demuth, Surf. Sci. **54**, 419 (1976).
[13] M. Van Hove, S. Y. Tong, and N. Stoner, Surf. Sci. **54**, 259 (1976).
[14] S. Hüfner, *Photoelectron Spectroscopy* (Springer, Berlin, 1995).
[15] *Angle-Resolved Photoemission*, edited by S. D. Kevan (Elsevier, Amsterdam, 1992).
[16] J. Osterwalder, P. Aebi, R. Fasel, D. Naumovic, P. Schwaller, T. Kreutz, L. Schlapbach, T. Abukawa, and S. Kono, Surf. Sci. **331–333**, 1002 (1995).
[17] J. O. Porteus, Surf. Sci. **41**, 515 (1974).
[18] R. Fischer, Th. Fauster, and W. Steinmann, Phys. Rev. B **48**, 15 496 (1993).
[19] N. Memmel and E. Bertel, Phys. Rev. Lett. **75**, 485 (1995).
[20] K. A. H. German, C. B. Weare, P. R. Varekamp, J. N. Andersen, and J. A. Yarmoff, Phys. Rev. Lett. **70**, 3510 (1993).
[21] K. Horn, J. Somers, Th. Lindner, and A. M. Bradshaw, in *Physics and Chemistry of Alkali Metal Adsorption* (Ref. 1).
[22] J. Küppers, in *Physics and Chemistry of Alkali Metal Adsorption* (Ref. 1).
[23] H. J. Levinson, F. Greuter, and E. W. Plummer, Phys. Rev. B **27**, 727 (1983).
[24] P. O. Gartland and B. J. Slagsvold, Solid State Commun. **25**, 489 (1978).
[25] G. V. Hansson and S. A. Flodström, Phys. Rev. B **18**, 1562 (1978).
[26] M. Heinrichsmeier, A. Fleszar, and A. G. Eguiluz, Surf. Sci. **285**, 129 (1993).
[27] E. V. Chulkov and V. M. Silkin, Surf. Sci. **215**, 385 (1989).